Original article

Folia Neuropathologica

A spatial pattern analysis of β-amyloid (Aβ) deposition in the temporal lobe in Alzheimer's disease

Richard A. Armstrong

Vision Sciences, Aston University, Birmingham B4 7ET, UK

Folia Neuropathol 2010; 48 (2): 67-74

Abstract

To determine the factors influencing the distribution of β-amyloid (Aβ) deposits in Alzheimer's disease (AD), the spatial patterns of the diffuse, primitive, and classic Aβ deposits were studied from the superior temporal gyrus (STG) to sector CA4 of the hippocampus in six sporadic cases of the disease. In cortical gyri and in the CA sectors of the hippocampus, the Aβ deposits were distributed either in clusters 200-6400 μm in diameter that were regularly distributed parallel to the tissue boundary or in larger clusters greater than 6400 μm in diameter. In some regions, smaller clusters of Aβ deposits were aggregated into larger 'superclusters'. In many cortical gyri, the density of Aβ deposits was positively correlated with distance below the gyral crest. In the majority of regions, clusters of the diffuse, primitive, and classic deposits were not spatially correlated with each other. In two cases, double immunolabelled to reveal the Aβ deposits and blood vessels, the classic Aβ deposits were clustered around the larger diameter vessels. These results suggest a complex pattern of Aβ deposition in the temporal lobe in sporadic AD. A regular distribution of Aβ deposit clusters may reflect the degeneration of specific cortico-cortical and cortico-hippocampal pathways and the influence of the cerebral blood vessels. Large-scale clustering may reflect the aggregation of deposits in the depths of the sulci and the coalescence of smaller clusters.

Key words: *Alzheimer's disease (AD), β-amyloid (Aβ) deposits, spatial pattern, clustering, blood vessels, cortico-cortical pathways.*

Introduction

β-amyloid (Aβ) deposition in the form of diffuse ('pre-amyloid'), primitive ('neuritic'), and classic ('dense-cored') deposits is a hallmark pathological feature of Alzheimer's disease (AD) [5,8,17,19]. In the cerebral cortex in AD, the Aβ deposits frequently occur in clusters that exhibit a regular periodicity parallel to the pia mater [14]. The factors that determine the clustering of Aβ deposits in AD, however, are largely unknown. Previous studies have suggested that Aβ deposits may aggregate within the sulci of adjacent gyri [3], in association with the columns of cells associated with specific anatomical projections [14], or in relation to the cerebral microcirculation [9,15]. The objective of the present study was to determine the spatial patterns of the diffuse, primitive, and classic Aβ deposits throughout the temporal lobe to address the following questions: 1) how are the individual Aβ deposit subtypes distributed, 2) is large-scale clustering of the Aβ deposits related to dif-

Communicating author:

Dr. R.A. Armstrong, Vision Sciences, Aston University, Birmingham B4 7ET, UK, phone 0121-359-3611, fax 0121-333-4220, e-mail: R.A.Armstrong@aston.ac.uk

ferential deposition within cortical sulci, 3) is smaller-scale clustering related to the anatomical connections of the temporal lobe, and 4) are the clusters of Aβ deposits spatially related to each other and/or to the cerebral microcirculation?

Material and methods

Cases

Six cases of sporadic AD (details in Table I) were obtained from the Brain Bank, Department of Neuropathology, Institute of Psychiatry, King's College, London, UK. Informed consent was given for the removal of all brain tissue according to the 1996 Declaration of Helsinki (as modified Edinburgh, 2000). Patients were clinically assessed and all fulfilled the 'National Institute of Neurological and Communicative Disorders and Stroke and the Alzheimer Disease and Related Disorders Association' (NINCDS/ADRDA) criteria for probable AD [29]. The histological diagnosis of AD was established by the presence of widespread neocortical senile plaques (SP) consistent with the 'Consortium to Establish a Registry of Alzheimer Disease' (CERAD) criteria [25]. All cases had an apolipoprotein E genotype of 3/4.

Histological methods

A coronal section of the complete temporal lobe (Fig. 1) was taken from each case at the level of the lateral geniculate body. Sections, 7 µm in thickness, were immunolabelled with a rabbit polyclonal antibody (Gift of Prof. B.H. Anderton) raised against the 12-28 amino acid sequence of the Aβ protein [28] to reveal the Aβ deposits. The antibody was used at a dilution of 1 in 1200 and incubated at 4° overnight. Sections were pretreated with 98% formic acid for 6 minutes to enhance immunoreactivity. Aβ was visualised using the streptavidin-biotin horseradish peroxidase procedure with diaminobenzidine as the chromogen. In two of the cases, sections were double immunolabelled with Aβ and collagen type IV antiserum (Europath Ltd, UK) to reveal the blood vessel profiles [9,23,24]. The antiserum was used at 1 : 500 dilution following protease digestion of the section with a solution of 0.04% pepsin. Collagen type IV stains a component of the cerebrovascular basement membrane [32] and hence, reveals arterioles, venules, precapillaries, and capillaries [9]. The three most common morphological types of Aβ deposit (Fig. 2) were identified using previously published criteria [5,17]. Hence, diffuse deposits were 10-200 µm in diameter, irregular in shape with diffuse boundaries and lightly immunlabelled; primitive deposits were 20-60 µm well demarcated, more symmetrical in shape; and strongly immunolabelled, and classic deposits were 20-60 µm had a distinct strongly immunolabelled central core surrounded by a more lightly immunolabelled 'corona' of dystrophic neurites.

Morphometric methods

The spatial distribution of the Aβ deposits was studied in each gyrus of the temporal lobe and in the CA sectors of the hippocampus of each AD case (Fig. 1): the superior temporal gyrus (STG), middle temporal gyrus (MTG), inferior temporal gyrus (ITG), lateral occipitotemporal gyrus (LOT), parahippocampal gyrus (PHG)/subiculum, and the CA sectors of the hippocampus. Aβ deposition was studied using

Table I. Demographic details, cause of death, post-mortem delay, and apolipoprotein E genotype of the Alzheimer disease cases studied

Case	Gender	Age	Onset	Cause of death	PM delay	Apo E
A	M	86	83	Bronchopneumonia	75	3/4
B	F	85	80	Bronchopneumonia	–	3/4
C	F	93	91	Bronchopneumonia	66	3/4
D	F	88	72	Bronchopneumonia	80	3/4
E	F	81	77	Bronchopneumonia	17	3/4
F	F	91	85	Bronchopneumonia	46	3/4

M – male, F – female, PM – post-mortem, Apo E – Apolipoprotein E genotype

1000 x 200 µm contiguous sample fields; the short dimension of the field (200 µm) being aligned with the surface of the pia mater. In the cerebral cortex, the long dimension of the field (1000 µm) included laminae I, II, and most of lamina III; the region containing the highest densities of Aβ deposits in AD [13]. The sample fields were extended from the PHG/subiculum into the hippocampus, the fields aligned at first with the alveus to sample sectors CA1 to CA3. Sampling was then continued into sector CA4 using a guideline marked on the slide and which ceased approximately 400 µm from the dentate gyrus fascia. An eye-piece micrometer with grid lines at intervals of 10 µm was used as the sample field. The number of diffuse, primitive, and classic Aβ deposits was counted in each sample field. In the two cases double immunolabelled to reveal the Aβ deposits and blood vessels, the frequency of the larger diameter (> 10 µm) blood vessels in a field was estimated by 'lattice sampling', i.e., by counting the number of times a vessel profile intersected the grid lines of the field [6].

Statistical analysis

The spatial pattern of the Aβ deposits, i.e., whether they were distributed randomly, regularly, or in clusters was analysed in each region using spatial pattern analysis [1,10,11]. Departure of a lesion from randomness can be measured by calculating the variance/mean (V/M) ratio of the lesion counts in a series of contiguous sample fields. If a lesion is randomly distributed, then the V/M ratio corresponds to a Poisson distribution and will approximate to unity. A V/M ratio less than unity indicates a regular distribution and greater than unity a clumped or clustered distribution. If a lesion is clustered, to determine the mean size of the clusters and whether the clusters are randomly or regularly distributed, counts of lesions in adjacent sample fields are added together successively to provide data for increasing field sizes, e.g., 200 × 1000 µm, 400 × 1000 µm, 800 × 1000 µm etc., up to a size limited by the length of the strip sampled. The V/M ratio is calculated at each stage and plotted against field size. A V/M peak indicates the presence of regularly spaced clusters and an increase in V/M to an asymptote the presence of randomly distributed clusters. Location of the peak indicates the mean cluster size. The statistical significance of a V/M peak was tested using the 't' distribution [4,10]. The spatial patterns were classified according to whether they were random, regular, or clustered. If clustered, the lesions were assigned to

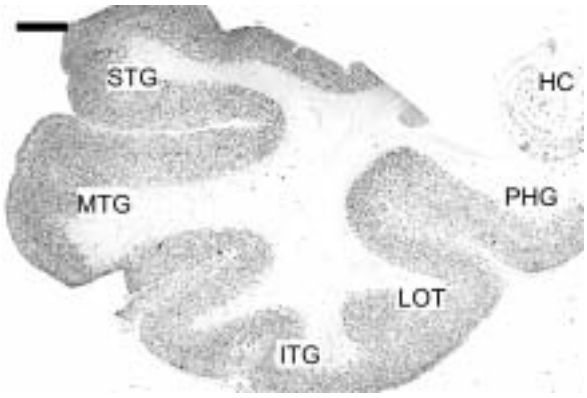

Fig. 1. Coronal section through the temporal lobe in a case of sporadic Alzheimer's disease showing the regions analysed: superior temporal gyrus (STG), middle temporal gyrus (MTG), inferior temporal gyrus (ITG), lateral occipitotemporal gyrus (LOT), parahippocampal gyrus (PHG), and the CA sectors of the hippocampus (HC) (section immunolabelled with $A\beta_{12-28}$, Haematoxylin; Magnification bar = 1.5 mm).

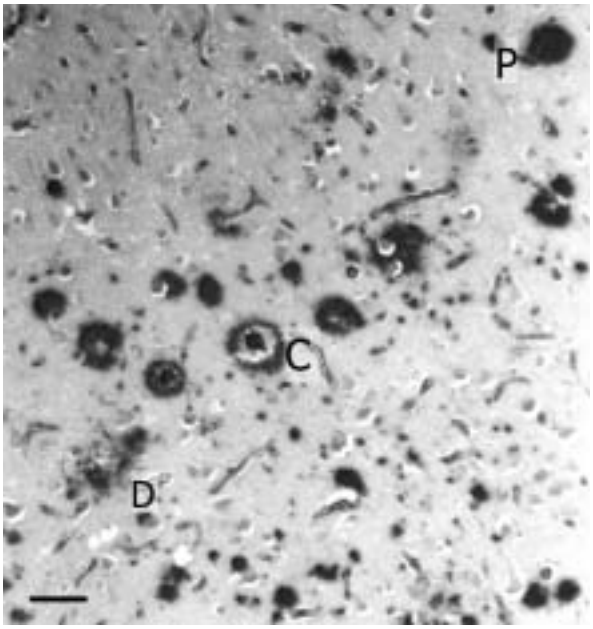

Fig. 2. The morphological types of β-amyloid (Aβ) deposit in the superior temporal gyrus of a case of sporadic Alzheimer's disease: Diffuse deposit (D), Primitive deposit (P), and Classic deposit (C) (Section immunolabelled with $A\beta_{12-28}$, Haematoxylin; Magnification bar = 50 µm).

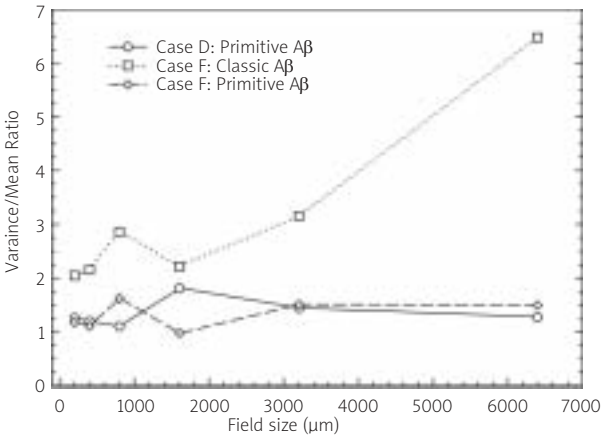

Fig. 3. The spatial distribution of individual types of β-amyloid (Aβ) deposit in specific brain regions of the temporal lobe in cases of Alzheimer's disease as revealed by spatial pattern analysis. Asterisks indicate significant V/M peaks.

two clustering patterns: 1) regularly spaced clusters 200 to 6400 µm in diameter arranged parallel to the tissue boundary and 2) large-scale clusters with a diameter of at least 6400 µm and without evidence of a regular distribution parallel to the tissue boundary. The frequency of cortical regions in which the size of regularly distributed clusters of deposits were in the range 400-800 µm, approximating to the dimension of the columns of neurons forming the cortico-cortical connections [20], was also determined.

Third, to determine whether aggregations of Aβ deposits were preferentially located on the crests of the gyri or within the sulci, the correlation between the counts of the Aβ deposits and distance below the gyral crest was tested at each field size for each gyrus. The spatial correlation between the counts of the diffuse, primitive, and classic Aβ deposits was also tested for each region. In addition, the correlation between the counts of Aβ deposits and the frequency of contacts with the blood vessel profiles was tested in two cases [7]. All correlations were tested using Pearson's correlation coefficient ('r').

Results

Examples of the spatial patterns exhibited by the Aβ deposits in individual gyri of the temporal lobe are shown in Fig. 3. In case D, the primitive deposits in the STG exhibited two V/M peaks, viz., at field sizes 200 µm and 1600 µm suggesting the presence of small, regularly distributed clusters of deposits 200 µm in diameter aggregated into larger 'superclusters' 1600 µm in diameter. In case F, the classic deposits in the MTG and the primitive deposits in the STG both exhibited a V/M peak at a field size of 800 µm suggesting a regular distribution of clusters of 800 µm in diameter arranged parallel to the pia mater.

The spatial patterns of the Aβ deposits in all cases and regions studied are summarised in Table II. In cortical gyri, the diffuse deposits were distributed in regular clusters in 13/30 (43%) gyri and in large clusters greater than 6400 µm in diameter in 14/30 (47%) gyri. In three of the gyri exhibiting regular clustering, the clusters were in the size range 400-800 µm. Primitive deposits were distributed in regular clusters in 20/30 (67%) gyri and in large clusters in 9/30 (30%) gyri. In eight gyri exhibiting regular clustering, the

Table II. The frequency of the different types of spatial patterns (R – Random distribution, Reg – Regular or uniform distribution) exhibited by β-amyloid (Aβ) deposits in cortical gyri and hippocampus (sectors CA1-4) of the temporal lobe in six cases of sporadic Alzheimer's disease (AD). Data in parentheses indicate the number of gyri in which the cluster size was in the range 400-800 µm

		Frequency of spatial pattern			
Region	Aβ deposit subtype	R	Reg	Regular clusters 200-6400 µm	Large clusters (> 6400 µm)
Cerebral cortex	Diffuse	4	1	13 (3)	12
	Primitive	1	0	20 (8)	9
	Classic	1	0	16 (10)	13
Hippocampus (CA1-4)	Diffuse	0	0	2 (1)	2
	Primitive	0	0	1 (1)	3
	Classic	1	0	2 (0)	2

clusters were in the size range 400-800 µm. Classic deposits were distributed in regular clusters in 16/30 (53%) gyri, and in large clusters in 13/30 (43%) gyri. In ten gyri exhibiting regular clustering, the clusters were in the size range 400-800 µm. A regular distribution of the clusters of diffuse, primitive, or classic deposit was also present in the hippocampus in 5/13 (38%) of analyses. In all regions, clustering at more than one scale, representing the aggregation of smaller clusters into 'superclusters', was present in 5/34 (15%) of analyses of the diffuse deposits, 5/34 (15%) analyses of the primitive deposits, and 5/35 (14%) of the classic deposits.

Correlations between the counts of Aβ deposits and distance below the gyral crest is shown in Table III. The diffuse Aβ deposits were positively correlated with distance below the gyral crest in 14/30 (47%) gyri, negatively correlated in 4/30 (13%) gyri, and not significantly correlated with distance in 12/30 (40%) gyri. The primitive Aβ deposits were positively correlated with distance below gyral crest in 12/30 (40%) gyri and not significantly correlated with distance in 18/30 (60%). The classic Aβ deposits were positively correlated with distance below the gyral crest in 10/30 (33%) gyri, negatively correlated in 1/30 (3%) gyri, and not significantly correlated with distance in 19/30 (63%) gyri.

Spatial correlations between the counts of the diffuse, primitive, and classic Aβ deposits are shown in Table IV. The diffuse and primitive deposits were negatively correlated in 5/36 (14%) regions and positively correlated in 2/36 (6%) regions studied. In addition, the diffuse and classic deposits were positively correlated in 2/34 (6%) regions, and negatively correlated in 1/34 (3%) regions. There were no significant correlations between the densities of the primitive and classic deposits.

Spatial correlations between the counts of Aβ deposits and the frequency of contacts with blood vessels in two of the cases is shown in Table V. In case A, there was a positive correlation between the classic deposits and blood vessels in the STG and MTG and in case F in the STG and PHG. No spatial correlations were observed between the diffuse and primitive type of deposits and the blood vessels.

Discussion

Spatial pattern analysis suggests that Aβ deposition occurred throughout the temporal lobe from the

Table III. Spatial correlations (Pearson's 'r') between the densities of the diffuse, primitive, and classic β-amyloid (Aβ) deposits in various cortical gyri: superior temporal gyrus (STG), middle temporal gyrus (MTG), inferior temporal gyrus (ITG), lateral occipitotemporal gyrus (LOT), parahippocampal gyrus (PHG), and distance below the gyral crest in six cases of Alzheimer's disease (AD)

		Aβ deposit subtype		
Case	Region	Diffuse	Primitive	Classic
A	STG	0.41***	0.27***	0.30***
	MTG	–0.35*	0.01	0.19
	ITG	0.54***	0.47***	–0.01
	LOT	0.05	–0.06	0.52***
	PHG	0.69***	0.54***	0.29*
B	STG	0.03	–0.08	0.05
	MTG	0.25*	–0.04	0.22
	ITG	0.10	0.13	0.21
	LOT	0	–0.20	–0.33**
	PHG	0.13	0	0.27**
C	STG	–0.22*	–0.09	0.34***
	MTG	0.27*	–0.08	–0.18
	ITG	0.48***	0.14	0.11
	LOT	–0.37**	0.46***	0.35**
	PHG	0.11	0.46**	0
D	STG	0.35***	0.05	0.08
	MTG	0.44***	0.08	–0.02
	ITG	0.22*	0.16	0.10
	LOT	–0.29**	–0.03	–0.16
	PHG	–0.09	0.36*	0.08
E	STG	0.17	0.28**	0.31***
	MTG	0.46***	0.21*	0.44***
	ITG	0.37***	0.29**	0.15
	LOT	–0.12	0.44*	0.32
	PHG	0.67***	–0.11	–0.01
F	STG	–0.08	0.15	–0.11
	MTG	0.04	-0.16	–0.01
	ITG	0.11	0.22	0.39***
	LOT	0.33**	0.45***	0.15
	PHG	0.29**	0.32**	0.32**

*$P < 0.05$, **$P < 0.01$, ***$P < 0.001$

Table IV. Frequency of spatial correlations (Pearson's 'r') between the densities of the diffuse, primitive, and classic β-amyloid (Aβ) deposits in various areas of the temporal lobe in six cases of sporadic Alzheimer's disease (AD)

Frequency of correlation				
Correlation	N	+ correlation	– correlation	NS
Diffuse/Primitive	36	2	5	29
Diffuse/Classic	34	2	1	31
Primitive/Classic	34	0	0	34

N – total number of regions analysed, NS – no significant correlation

Table V. Spatial correlations (Pearson's 'r') between the densities of the diffuse, primitive, and classic β-amyloid (Aβ) deposits and the frequency of large diameter (> 10 µm) blood vessels in various regions of the temporal lobe: superior temporal gyrus (STG), middle temporal gyrus (MTG), inferior temporal gyrus (ITG), lateral occipitotemporal gyrus (LOT), parahippocampal gyrus (PHG), and the CA sectors of the hippocampus, in two cases of sporadic Alzheimer's disease

		Aβ deposit subtype		
Case	Region	Diffuse	Primitive	Classic
A	STG	–0.05	–0.10	0.20*
	MTG	–0.12	–0.10	0.38***
	ITG	–0.14	–0.18	–0.03
	LOT	–0.09	–0.10	–0.12
	PHG	–0.07	0.03	0.10
	CA1/4	–	–	–
F	STG	0.09	–0.02	0.27*
	MTG	–0.05	–0.08	0.14
	ITG	0.10	0.12	0.09
	LOT	0.12	0.03	–0.05
	PHG	0.12	0	0.23*
	CA1/4	–0.03	–0.13	–0.06

**P < 0.05, ***P < 0.001*

STG to sector CA4 of the hippocampus [14]. Large aggregations of Aβ deposits with a diameter greater than 6400 µm occur within many individual gyri. Hence, the data support the hypothesis that the temporal lobe is one of the regions most significantly affected by Aβ pathology in sporadic AD [13,16,26].

Two types of spatial pattern were commonly observed within individual regions: 1) Aβ deposits were distributed in clusters 200-6400 µm in diameter that were regularly distributed parallel to the tissue boundary or 2) the deposits were distributed in much larger clusters greater than 6400 µm; a single large cluster often being present within the gyrus. These results are similar to those reported previously in AD [14] and also similar to those reported for neurofibrillary tangles (NFT) in AD [2,12]. A regular distribution of clusters of deposits parallel to the pia mater or alveus suggests a relationship with the functional connections of the cortex and hippocampus. In the cerebral cortex, the cells of origin of the cortico-cortical projections are clustered and occur in bands which are distributed along the cortical ribbon. Individual bands of cells vary in width approximately from 400-500 µm to 800-1000 µm depending on cortical area [20]. In some gyri, the estimated widths of the clusters of Aβ deposits were within this size range which suggests an association with these projections [26]. In the remaining regions, clusters of Aβ deposits were significantly larger than the size range of the cortico-cortical modules. The relationship between Aβ deposition and the cortico-cortical pathways could vary at different stages of the disease. Early in the disease, small clusters of Aβ deposits may occur in association with specific cortico-cortical projections but as the disease progresses, subsequent Aβ formation may result in the coalescence of the original clusters.

In many areas, large clusters of deposits > 6400 µm were observed. In a proportion of cortical gyri, significant correlations were observed between the density of Aβ deposits and distance below the crest of the gyrus. In a few gyri, there was a greater accumulation of deposits within the crest of the gyrus but most commonly, the density of deposits was greater in the depths of the gyri. The density of neurons and blood vessels is often greater in sulci compared with the gyral crest which could explain these accumulations [3,18]. Hence, aggregation of deposits within sulci is one explanation for the larger-scale clustering of Aβ deposits observed in gyri of the temporal lobe in AD.

In addition, in some regions, small regularly distributed clusters of Aβ deposits were themselves aggregated into larger 'superclusters'. Clustering at different 'scales' suggests a complex relationship between Aβ deposition and the underlying anatomical structure of the temporal lobe. For example, in the cerebral cortex, small-scale clustering could represent Aβ deposition in association with individual cortical modules and the 'superclusters' with groups of modules associated with a specific pathway. In addition, it may reflect the possibility that smaller clusters of Aβ deposits may become aggregated into larger accumulations as the disease progresses [2,8].

Different Aβ deposit subtypes could represent stages in the maturation of a single deposit type [5]. Hence, the diffuse deposits may represent the earliest stage of Aβ pathology and evolve into the primitive and classic deposits as the disease progresses [5]. If within a large cluster of diffuse deposits, however, smaller clusters 'evolve' into primitive deposit, a negative spatial correlation between the diffuse and primitive deposits should be the result. Conversely, if evolution from diffuse to primitive deposits is more random within large clusters of diffuse deposits, a positive spatial correlation may result in the region as a whole. Few spatial correlations between subtypes were observed, however, suggesting that each Aβ deposit subtype is distributed relatively independently [5]. These data support the hypothesis that each Aβ deposit subtype has an independent origin and that its morphology reflects specific aspects of cortical structure [5]. Hence, diffuse deposits are associated with neuronal cell bodies, primitive deposits with dendritic degeneration, and classic deposits with blood vessels [5].

The classic type of Aβ deposit was the only subtype to exhibit a positive spatial correlation with the blood vessels [9,15]. The classic deposits were clustered around the larger diameter (> 10 μm) blood vessels and especially the vertically penetrating arterioles in the upper laminae [9]. This spatial pattern may reflect: 1) Aβ deposition in association with the basement membranes or smooth muscle of blood vessel walls [27,30,31], 2) the deposition of Aβ by axon terminals or reactive glial cells juxtaposed to vessel walls [21], or, 3) diffusion of substances from blood vessels [9]. Diffusion from vessels is a possible explanation since the number of classic deposits declines exponentially with distance from the vessel consistent with a diffusional process [9] and the classic deposits contain many molecular constituents, some of which may have originated from blood vessels [5]. In addition, blood vessels with collapsed or degenerated endothelia are evident in more than 90% of AD cases [22] and occur concurrently with Aβ deposition.

In conclusion, large accumulations of Aβ deposits occur within individual gyri of the temporal lobe in AD. Aggregation of Aβ deposits within sulci and coalescence of smaller clusters are likely to explain larger-scale clustering patterns. In addition, Aβ deposits exhibit a range of smaller-scale patterns including regularly distributed clusters of varying size, and smaller clusters aggregated into superclusters. Association of the Aβ deposits with the degeneration of specific anatomical connections and with the cerebral microcirculation could determine these spatial patterns.

Acknowledgements

Brain tissue sections used in this study were kindly provided by the Brain Bank, Deptartment of Neuropathology, Institute of Psychiatry, King's College London, UK.

References

1. Armstrong RA. The usefulness of spatial pattern analysis in understanding the pathogenesis of neurodegenerative disorders, with particular reference to plaque formation in Alzheimer's disease. Neurodegen 1993; 2: 73-80.
2. Armstrong RA. Is the clustering of neurofibrillary tangles in Alzheimer's patients related to the cells of origin of specific cortico-cortical projections? Neurosci Lett 1993; 160: 57-60.
3. Armstrong RA. Quantitative differences in β/A4 protein subtypes in the parahippocampal gyrus and frontal cortex in Alzheimer's disease. Dementia 1994; 5: 1-5.
4. Armstrong RA. Analysis of spatial patterns in histological sections of brain tissue. J Neurosci Meth 1997; 73: 141-147.
5. Armstrong RA. β-amyloid plaques: stages in life history or independent origin? Dement Geriatr Cogn Disord 1998; 9: 227-238.
6. Armstrong RA. Quantifying the pathology of neurodegenerative disorders: quantitative measurements, sampling strategies and data analysis. Histopathol 2003; 42: 521-529.
7. Armstrong R. Measuring the degree of spatial correlation between histological features in thin sections of brain tissue. Neuropathol 2003; 23: 245-253.
8. Armstrong RA. Plaques and tangles and the pathogenesis of Alzheimer's disease. Folia Neuropathol 2006; 44: 1-11.
9. Armstrong RA. Classic β-amyloid deposits cluster around large diameter blood vessels rather than capillaries in sporadic Alzheimer's disease. Curr Neurovasc Res 2006; 3: 289-294.
10. Armstrong RA. Methods of studying the planar distribution of objects in histological sections of brain tissue. J Microsc 2006; 221: 153-158.

11. Armstrong RA. Measuring the spatial arrangement patterns of pathological lesions in histological sections of brain tissue. Folia Neuropathol 2007; 44: 229-237.
12. Armstrong RA. Clustering and periodicity of neurofibrillary tangles in the upper and lower cortical laminae in Alzheimer's disease. Folia Neuropathol 2008; 46: 26-31.
13. Armstrong RA, Myers D, Smith CUM, Cairns NJ, Luthert PJ. Alzheimer's disease: the relationship between the density of senile plaques, neurofibrillary tangles and A4 deposits in human patients. Neurosci Letters 1991; 123: 141-143.
14. Armstrong R, Myers D, Smith C. The spatial patterns of β/A4 deposit subtypes in Alzheimer's disease. Acta Neuropathol 1993; 86: 36-41.
15. Armstrong R, Cairns N, Lantos P. Spatial distribution of diffuse, primitive, and classic amyloid-β deposits and blood vessels in the upper laminae of the frontal cortex in Alzheimer's disease. Alz Dis Assoc Disord 1998; 12: 378-383.
16. De Lacoste M, White CL III. The role of cortical connectivity in Alzheimer's disease pathogenesis: a review and model system. Neurobiol Aging 1993; 14: 1-16.
17. Delaere P, Duyckaerts C, He Y, Piette F, Hauw J. Subtypes and differential laminar distributions of β/A4 deposits in Alzheimer's disease: relationship with the intellectual status of 26 cases. Acta Neuropathol 1991; 81: 328-335.
18. Gentleman SM, Williams B, Roystan MC, Jagoe R, Clinton J, Perry RH, Ince PG, Allsop D, Polak JM, Roberts GW. Quantification of β/A4 protein deposition in the medial temporal lobe: A comparison of Alzheimer's disease and senile dementia of the Lewy Body Type. Neurosci Lett 1992; 142: 9-12.
19. Glenner GG, Wong CW. Alzheimer's disease and Down's syndrome: sharing of a unique cerebrovascular amyloid fibril protein. Biochem Biophys Res Commun 1984; 122: 1131-1135.
20. Hiorns RW, Neal JW, Pearson RCA, Powell TPS. Clustering of ipsilateral cortico-cortico projection neurons to area 7 in the rhesus monkey. Proc R Soc Lond 1991; 246: 1-9.
21. Kalaria R. The blood-brain barrier and cerebral microcirculation in Alzheimer disease. Cerebrovasc Brain Met Rev 1992; 4: 226-260.
22. Kalaria R, Hedera P. Differential degeneration of the cerebral microvasculature in Alzheimer's disease. NeuroReport 1995; 6: 477-480.
23. Kawai M, Kalaria R, Harik S, Perry G. The relationship of amyloid plaques to cerebral capillaries in Alzheimer's disease. Am J Pathol 1990; 137: 1435-1446.
24. Luthert P, Williams J. A quantitative study of the coincidence of blood vessels and A4 protein deposits in Alzheimer's disease. Neurosci Lett 1991; 126: 110-112.
25. Mirra S, Heyman A, McKeel D, Sumi S, Crain B, Brownlee L, Vogel F, Hughes J, van Belle G, Berg L. The consortium to establish a registry for Alzheimer's disease (CERAD). II. Standardisation of the neuropathological assessment of Alzheimer's disease. Neurology 1991; 41: 479-486.
26. Pearson RCA, Esiri MM, Hiorns RW, Wilcock GK, Powell TPS. Anatomical correlates of the distribution of the pathological changes in the neocortex in Alzheimer's disease. Proc Natl Acad Sci 1985; 82: 4531-4534.
27. Perlmutter L, Chui C. Microangiopathy, the vascular basement membrane and Alzheimer's disease: A review. Brain Res Bull 1990; 24: 677-686.
28. Spargo E, Luthert P, Anderton B, Bruce M, Smith D, Lantos P. Antibodies raised against different proteins of the A4 protein identify a subset of plaques in Down's syndrome. Neurosci Lett 1990; 115: 345-350.
29. Tierney M, Fisher R, Lewis A, Zorzitto M, Snow W, Reid D, Nieuwstraten P. The NINCDS-ADRDA work group criteria for the clinical diagnosis of probable Alzheimer's disease. Neurology 1988; 38: 359-364.
30. Wisniewski H, Wegiel J. β-amyloid formation by myocytes of leptomeningeal vessels. Acta Neuropathol 1994; 87: 223-241.
31. Yamaguchi H, Yamazaki T, Lemere C, Frosch M, Selkoe D. Beta-amyloid is focally deposited within the outer basement membrane in the amyloid angiopathy of Alzheimer's disease. Am J Pathol 1992; 141: 249-259.
32. Yurchenco P, Schittny J. Molecular architexture of basement membranes. FASEB J 1990; 4: 1577-1590.